Math. Model. Nat. Phenom.
Vol. 11, No. 5, 2016, pp. 119–136
DOI: 10.1051/mmnp/201611508

Modeling of Sensory Characteristics Based on the Growth of Food Spoilage Bacteria

D. Valenti[1*], G. Denaro[2], F. Giarratana[3], A. Giuffrida[3], S. Mazzola[2], G. Basilone[2], S. Aronica[2], A. Bonanno[2], B. Spagnolo[1,4,5]

[1] Dipartimento di Fisica e Chimica, Università di Palermo, Group of Interdisciplinary Theoretical Physics and CNISM, Unità di Palermo, Viale delle Scienze, Ed. 18, I-90128 Palermo, Italy

[2]Istituto per l'Ambiente Marino Costiero, CNR, U.O.S. di Capo Granitola, Via del Faro 3, I-91020 Campobello di Mazara (TP), Italy

[3] Dipartimento di Scienze Veterinarie, Università di Messina, Polo Universitario dell'Annunziata, 98168 Messina, Italy

[4]Radiophysics Department, Lobachevsky State University, Nizhniy Novgorod, Russia

[5] Istituto Nazionale di Fisica Nucleare, Sezione di Catania, Italy

Abstract. During last years theoretical works shed new light and proposed new hypothesis on the mechanisms which regulate the time behaviour of biological populations in different natural systems. Despite of this, a relevant physical and biological issue such as the role of environmental variables in ecological systems is still an open question. Filling this gap of knowledge is a crucial task for a deeper comprehension of the dynamics of biological populations in real ecosystems.

The aim of this work is to study how dynamics of food spoilage bacteria influences the sensory characteristics of fresh fish specimens. This topic is worth of investigation in view of a better understanding of the role played by the bacterial growth on the organoleptic properties, and becomes crucial in the context of quality evaluation and risk assessment of food products. We therefore analyze and reproduce the time behaviour, in fresh fish specimens, of sensory characteristics starting from the growth curves of two spoilage bacterial communities.

The theoretical study, initially based on a deterministic model, is performed by using the temperature profiles obtained during the experimental analysis. As a first step, a model of predictive microbiology is used to reproduce the experimental behaviour of the two bacterial populations. Afterwards, the theoretical bacterial growths are converted, through suitable differential equations, into "sensory" scores, based on the Quality Index Method (QIM), a scoring system for freshness and quality sensory estimation of fishery products. As a third step, the theoretical curves of QIM scores are compared with the experimental data obtained by sensory analysis. Finally, the differential equations for QIM scores are modified by adding terms of multiplicative white noise, which mimics the effects of uncertainty and variability in sensory analysis. A better agreement between experimental and theoretical QIM scores is observed, in some cases, in the presence of suitable values of noise intensity respect to the deterministic analysis.

Keywords and phrases: population dynamics, predictive microbiology, stochastic ordinary differential equations

Mathematics Subject Classification: 82C05, 92D25, 92D40, 60H10

1. Introduction

In this work we review a recent result [35] obtained in the context of predictive microbiology [5, 18, 69] (a theoretical approach to describe microbial dynamics in food products) and sensory analysis (a tool which permits to evaluate the food quality through sensory indicators). The previous study, based on a deterministic model, which allowed to reproduce experimental findings for fresh fish specimens, is deepened by improving fitting procedures and statistical analysis.
We recall here that the general idea of predictive microbiology is to model the dynamics of microbial populations, in particular bacteria, responsible for food spoilage, taking into account the changes of environmental variables such as temperature (T), pH, and water activy (aw). Mathematical models can be therefore very useful for practical applications, since some food products, such as ripened meats and cheeses, are obtained under a continuous modification of T, pH (hydrogen ion concentration), and relative humidity (RH). For example, a class of models, devised to reproduce the bacterial dynamics in food products, exploits generalized Lotka-Volterra equations, which describe the time evolution of two different microbial populations both in deterministic and stochastic regime [23, 32–34].
Predictive models are classified as primary, secondary and tertiary [69]. Primary models provide microbial dynamics. Secondary models describe the dynamics of environmental variables which appear in primary models. Finally, tertiary models combine primary and secondary models, allowing to take into account the effects of environmental variables on the microbial growth [18]. We note that the real bacterial growth can be overestimated if the competitive natural microflora is not taken into account by these models [5].
It is clear that the growth of spoilage bacteria in a fish product determines a loss of quality, which appears through a worsening of the sensory characteristics. These are "measured" by a scoring system for freshness and quality sensory estimation of fishery products, known as Quality Index Method (QIM) and initially developed by the Tasmanian Food Research Unit [11].
The QIM scoring allows to assign demerit points to each sensory parameter considered, providing by a summation of the partial scores an overall sensory score, named Quality Index (QI).
A crucial point is how to relate the sensory characteristics of a fresh fish products to bacterial populations responsible for fish spoilage. This subject has been widely debated, since the sensory modifications in fish specimens is due to the growth of spoilage bacteria on skin, gills, and flesh [38, 41, 45]. These sites, in fact, are those taken into account by the sensory evaluation schemes such as QIM. However, the bacterial penetration through the skin can occur very slowly [31]. As a consequence the sensory modifications in a fresh fish specimens is expected to depend mainly on the spoilage bacteria located on skin and gills.
Because of this, to predict correctly the whole-fish freshness, one should model separately the dynamics of the specific spoilage bacteria (SSB) on skin, gills, and flesh [35].
Here we analyze the connection between sensory characteristics of fresh fish specimens and two bacterial populations responsible for fish spoilage. The sensory characteristics are "measured" by the QIM scoring system [11].
The analysis consists in a theoretical study, initially based on a set of deterministic differential equations for bacterial dynamics and QIM scores, which allows: i) to model the experimental behaviour of two SSB populations, obtained separately on skin, gills and flesh under different storage conditions, i.e. varying the temperature; ii) to reproduce the QI scores, obtained for Gilthead seabream (*Sparus aurata*) specimens, starting from the theoretical bacterial curves obtained at the previous step.
It is important to recall that environmental perturbations can affect significantly the dynamics of real physical and biological systems [15, 16, 44, 50, 52, 58]. In particular, the interplay between fluctuations and nonlinearity in physical, biological, and social systems as well as in financial markets can give rise to counterintuitive phenomena, such as stochastic resonance, noise enhanced stability, resonant activation, noise delayed extinction, enhanced stochastic temporal and spatio-temporal oscillations, effects of intrinsic noise, induced chaotic transitions from periodic attractors, and pattern formation [1–3, 6–10, 12–14, 17, 19, 20, 24–30, 36, 37, 40, 42, 43, 46–48, 51, 55–57, 59–64, 66, 67]. Variability of environmental parameters,

*Corresponding author. E-mail: davide.valenti@unipa.it

such as temperature and food availability, influence the dynamics of real biological systems, favouring the survivance of some populations and contributing to the extinction of other ones.
Natural systems are open systems, because of their continuous interaction with the environment, which influences their dynamics by deterministic and random perturbations. Moreover, natural systems are governed by nonlinear dynamics. These two characteristics, i.e. nonlinearity and external random perturbations, make them complex systems, so that population dynamics, such as spatio-temporal dynamics of phytoplankton species in a marine ecosystem, has to be studied by stochastic approaches, which take into account the presence of random fluctuations [21, 22, 65, 68].
As a final step, we take therefore into account the effects of uncertainty and variability in sensory analysis, and modify the differential equation for QI scores by adding terms of multiplicative white noise. The stochastic model is solved for different values of noise intensities. The QI time behaviours obtained are compared with the experimental ones by calculating the root mean square error (RMSE). As a result, we find that some curves of theoretical QI scores, obtained in the presence of suitable noise intensities, are in a better agreement with those observed experimentally respect to those calculated by the deterministic model.

2. Experimental data

2.1. Fish specimens and storage conditions

Bacterial concentrations were obtained from Gilthead seabream (300 –500 g) raised in three Italian fish farms (farm 1, 2, and 3). After death the fish were subdivided in four groups and stored at different temperatures. Group 1 consisted of 147 fish subdivided in seven batches, each containing twenty-one specimens. This group was used to carry out seven replicated trials (three trials from farm 1, two from farm 2, and two from farm 3) in such a way to characterize the variability of the fish shelf life and to obtain a better parametrization for Eqs. (3.1)-(3.3) with particular regard to coefficients β_1 and β_2 (see Section 3).
Group 2 consisted of one batch of twenty-eight fish from farm 1, while Group 3, as well as Group 4, consisted of one batch of twenty-one fish, always coming from farm 1.
The storing temperature were monitored for all groups. Measures of bacterial concentrations and sensory evaluations were carried out after 0, 72, 168, 216, 336, 408 and 504 h from the beginning of storage, by sampling three fish for each time interval. Microbiological assays were performed by sampling, with sterile instruments, 10 g of dorsal skin, 5 g of gills, and 20 g of dorsal flesh; this last kind of sample was obtained from the opposite side where skin was sampled, rinsing the skin with 70% ethanol and removing the flesh aseptically.

2.2. Microbiological analyses and sensory evaluation

Microbiological analyses revealed the presence of two different bacterial populations, i.e. Pseudomonas spp. and Shewanella spp., recorded as sulphide non-producers (white colonies) and sulphide-producers (black colonies), respectively.
Sensory evaluation was carried out by using the QIM scheme developed for raw whole Gilthead seabream [38], considering variables connected with surface and eyes appearance, odour, elasticity of the muscle and gills, taking into account a maximum of 15 demerit points. The sensory evaluation was performed by an expert panel of three persons.

3. Deterministic model

The time behaviour of QIM parameters were obtained by modeling separately the dynamics of: i) QI_S, related to scores for surface/eyes appearance and odour (0–10 demerit points); ii) QI_G connected with gills scores (0–4 demerit points); iii) QI_F related to scores assigned to the flesh evaluation (0–1 demerit points). Our main hypothesis, based on previous studies (see Section 1), is that QI_S, QI_G and QI_F

depend on the bacterial counts performed on skin, gills and flesh, respectively, according to the following differential equations [35]

$$\frac{dQI_S}{dt} = \frac{dN_{wS}}{dt}\beta_{1S} + \frac{dN_{bS}}{dt}\beta_{2S} \tag{3.1}$$

$$\frac{dQI_G}{dt} = \frac{dN_{wG}}{dt}\beta_{1G} + \frac{dN_{bG}}{dt}\beta_{2G} \tag{3.2}$$

$$\frac{dQI_F}{dt} = \frac{dN_{wF}}{dt}\beta_{1F} + \frac{dN_{bF}}{dt}\beta_{2F}, \tag{3.3}$$

where $N_{wi}(t)$ and $N_{bi}(t)$ $(i = S, G, F)$ are the concentrations, expressed in Log CFU g^{-1}, of sulphide non-producers (white colonies) and sulphide-producers (black colonies) bacteria, respectively, at time t, on skin (S), gills (G) and flesh (F). Here CFU is an acronym for "colony forming units", whose value provides a measure of bacterial concentration, while β_1 and β_2 are two coefficients that convert the bacterial concentrations into demerit points. The bacterial concentrations $N_{wi}(t)$ and $N_{bi}(t)$ are modeled by the following differential equations [4]

$$\frac{dN_{wi}(t)}{dt} = \mu_w^{max}\, N_{wi}(t)\frac{Q_{wi}}{1+Q_{wi}}\left(1 - \frac{N_{wi}(t)}{N_{wi}^{max}(t)}\right) \tag{3.4}$$

$$\frac{dQ_{wi}}{dt} = \mu_w^{max}\, Q_{wi} \tag{3.5}$$

$$\frac{dN_{bi}(t)}{dt} = \mu_b^{max}\, N_{bi}(t)\frac{Q_{bi}}{1+Q_{bi}}\left(1 - \frac{N_{bi}(t)}{N_{bi}^{max}}\right) \tag{3.6}$$

$$\frac{dQ_{bi}}{dt} = \mu_b^{max}(t)\, Q_{bi}, \tag{3.7}$$

where μ_w^{max} and μ_b^{max} are the maximum specific growth rates of the white and black population, respectively. N_{wi}^{max} and N_{bi}^{max} $(i = S, G, F)$ are the theoretical maximum population densities of the white and black population, respectively, on skin, gills and flesh under monospecific growth conditions, that is in the absence of interspecific interaction. Finally, Q_{wi} and Q_{bi} $(i = S, G, F)$ are the physiological states of the white and black population, respectively, on skin, gills and flesh. We note that the physiological state, which represents the state of bacterial life functions, plays a crucial role in the whole microbial dynamics, since it measures how efficient the bacterial metabolism is and, as a consequence, determines the values of growth rate. Specifically, maximum growth rates of Pseudomonas spp. and Shewanella spp. were calculated according to Refs. [49, 53, 54], modified as described below

$$\mu_w^{max} = \exp[b_0 + b_1\, T + b_2\, pH + b_3\, T\, pH + b_4\, T^2 + b_5\, pH^2] \tag{3.8}$$

$$\mu_b^{max} = [c_0\,(T + c_1)]^2. \tag{3.9}$$

Here, the values of the parameters in Eqs. (3.8), (3.9) are $b_0 = -12.4$, $b_1 = 0.03318$, $b_2 = 2.948013$, $b_3 = 0.011715$, $b_4 = 0.004123$, $b_5 = -0.25717$, and $c_0 = 0.027$, $c_1 = 2.08$, respectively. These parameters were obtained by fitting data for specific growth under different constant values of temperature and pH.

4. Results and discussion

4.1. Bacterial dynamics

As a first step, we solved Eqs. (3.4)-(3.7) by using: i) secondary models given by Eqs. (3.8), (3.9), where pH is set at a constant value (pH=7.0); ii) initial values, N_{wi}^0 and N_{bi}^0, and theoretical maximum population concentrations, N_{wi}^{max} and N_{bi}^{max}, obtained by experimental data. Moreover, to fix Q_{wi}^0 and Q_{bi}^0 (initial values of the physiological states) we used a fitting procedure based on the minimization of the distance between experimental and theoretical curves for bacterial concentrations, i.e. the minimum of

the root mean square error (RMSE). By this way, we obtained the theoretical curves for the two bacterial concentrations in the three different sites (skin, gills, flesh).
We note that this procedure was performed by using separately bacterial concentration data from Group 1, Group 2, Group 3, and Group 4. As a result, for each site and each population, we obtained one experimental growth curve as an average over the replicated trials carried out in each group, and correspondingly one theoretical curve (green line), which are shown in Figs. 1-4, together with the profile of temperature (red line) expressed in $^{\circ}C$.

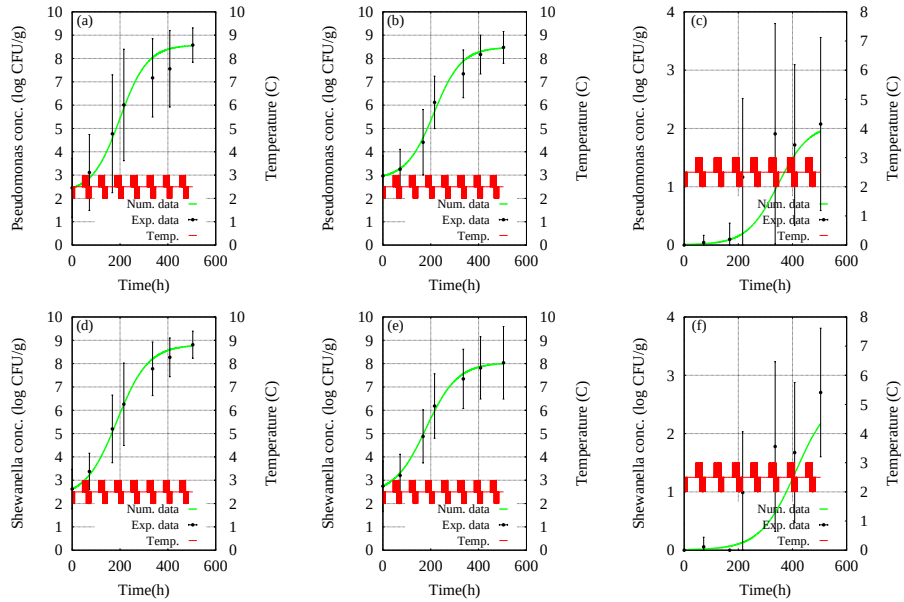

FIGURE 1. *Group 1. Comparison between experimental data (black dots) and theoretical curves (green line) of bacterial growth: Pseudomonas (white colonies) in panels a (skin), b (gills), c (flesh); Shewanella (black colonies) in panels d (skin), e (gills), f (flesh). Vertical bars indicate experimental errors. Red curves represent the temperature profiles.*

Here we observe that, in general, the time behaviours of Pseudomonas (white colonies) and Shewanella (black colonies) are comparable for all groups.
More precisely, the initial concentrations of white and black colonies, on skin and gills, were rather low (<Log 3 CFU g^{-1}), but the flesh maintained a bacterial load even smaller (<Log 1 CFU g^{-1}) until the 72^{nd} hour.
Moreover, the growth of both bacterial populations on skin and gills was similar in all groups. In particular, in Groups 2, 3 and 4, the growth was faster, and determined after 168–216 h a concentration <Log 8 CFU g^{-1}. Conversely, the bacterial load in the flesh was characterized by values < Log 4.5 CFU g^{-1}. These results confirm that skin and gills are the sites where the bacterial growth occurs more quickly [39].

4.2. Prediction of QI values

As a second step, we focused on data from Group 1, by using Eqs. (3.1)-(3.3) to convert theoretical bacterial concentrations of this group (see green curves in Fig. 1) into QI values. As initial conditions, QI_S^0, QI_G^0, and QI_F^0, we used those obtained by sensory analysis.
Moreover, analogously to the procedure adopted to set Q_{wi}^0 and Q_{bi}^0, we fixed the values of conversion coefficients ($\beta_{1S} = 0.01 \pm 0.01$, $\beta_{2S} = 1.39 \pm 0.01$, $\beta_{1G} = 0.01 \pm 0.01$, $\beta_{2G} = 0.70 \pm 0.01$, $\beta_{1F} = 0.33 \pm 0.01$, $\beta_{2F} = 0.16 \pm 0.01$) by using a fitting procedure, based on the minimization of the RMSE between ex-

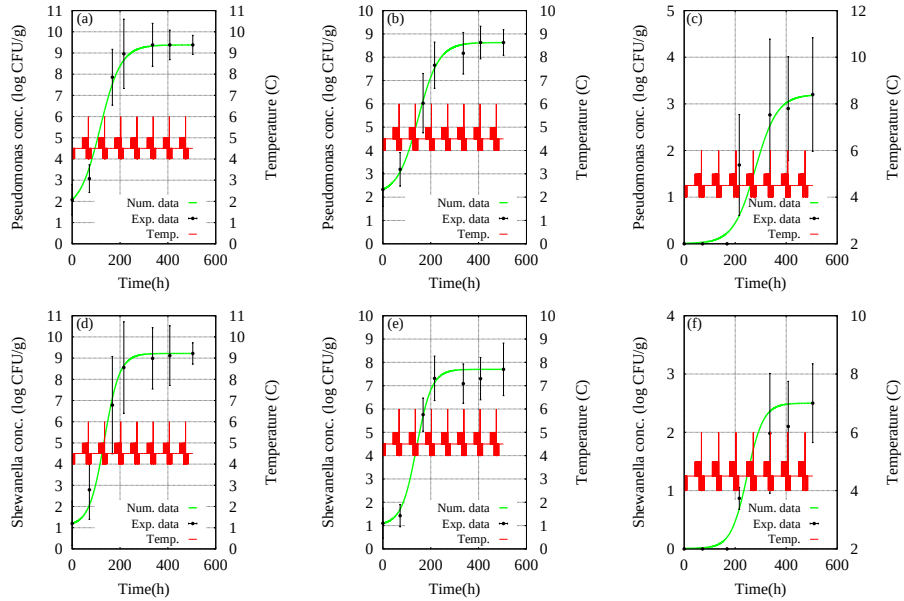

FIGURE 2. *Group 2. Comparison between experimental data (black dots) and theoretical curves (green line) of bacterial growth: Pseudomonas (white colonies) in panels a (skin), b (gills), c (flesh); Shewanella (black colonies) in panels d (skin), e (gills), f (flesh). Vertical bars indicate experimental errors. Red curves represent the temperature profiles.*

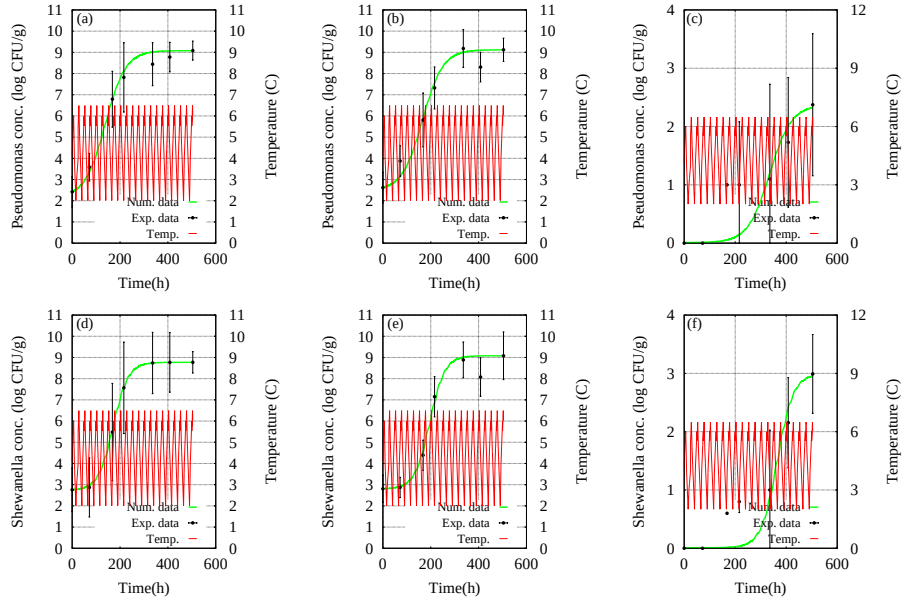

FIGURE 3. *Group 3. Comparison between experimental data (black dots) and theoretical curves (green line) of bacterial growth: Pseudomonas (white colonies) in panels a (skin), b (gills), c (flesh); Shewanella (black colonies) in panels d (skin), e (gills), f (flesh). Vertical bars indicate experimental errors. Red curves represent the temperature profiles.*

perimental data and theoretical curves of $QI_S(t)$, $QI_G(t)$, and $QI_F(t)$. By this way, we obtained the theoretical values of the quality index in the three different sites (skin, gills, flesh). Fig. 5 shows curves of $QI_S(t)$, $QI_G(t)$, and $QI_F(t)$ obtained by the model (green line), corresponding experimental values (black dots), and temperature profiles (red line). Specifically, panels a, b, and c display QIs for the three

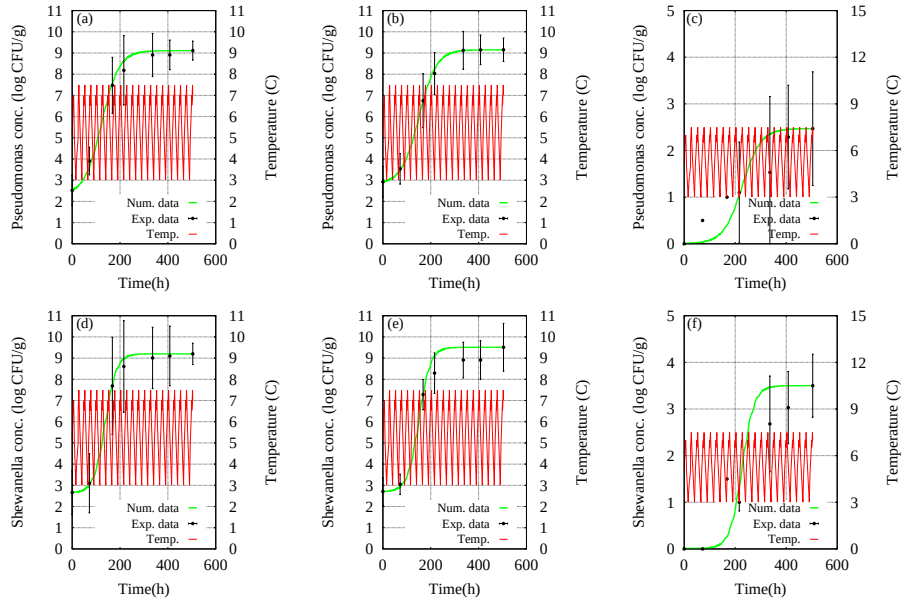

FIGURE 4. *Group 4. Comparison between experimental data (black dots) and theoretical curves (green line) of bacterial growth: Pseudomonas (white colonies) in panels a (skin), b (gills), c (flesh); Shewanella (black colonies) in panels d (skin), e (gills), f (flesh). Vertical bars indicate experimental errors. Red curves represent the temperature profiles.*

different sites, while panel d refers to the total QI score, defined as summation of the three partial quality indexes: $QI(t)$=$QI_S(t)$+$QI_G(t)$+$QI_F(t)$.

We recall that this procedure was performed by using uniquely data from Group 1. Accordingly, the values of β_{1i}, β_{2i} $(i = S, G, F)$ were obtained by performing the best fitting between predicted and observed QIs scores only for Group 1. We note also that the observed QIs values used here were obtained as averages over sensory evaluations performed by three expert persons. As a further step, we intend to show that the conversion coefficients β_{1i} and β_{2i}, obtained by using uniquely data from Group 1, can be used also for the other three groups. As a consequence, one should observe a general correspondence, mathematically expressed by Eqs. (3.1)-(3.3), between bacterial concentrations and predicted QIs. This correspondence should indicate that the "conversion" depends mostly on the bacterial species (and eventually strains), without being influenced by the specific dataset. At this aim, in the following we use the values of β_{1i}, β_{2i} $(i = S, G, F)$ calculated from Group 1 to predict QIs scores also for Groups 2, 3, 4. Results are given in Figs. 6-8, where sensory-analysis data (black dots), corresponding predicted values (green line), and temperature profiles (red line) are shown.
As one can expect, a good agreement between predicted and observed QIs scores of Group 1 (see Fig. 5) is found. Moreover, the model is also able to reproduce the time behaviour of quality indexes for Groups 2, 3, 4, even if the agreement between predicted and observed QIs scores is less good (see Figs. 6-8). This can be explained by noting that in all groups the theoretical bacterial growth was analyzed by assuming the presence of two populations, i.e. Shewanella and Pseudomonas. However, discrepancies in the composition of bacterial flora (both at level of species and strains) among the four groups can be present, and determine for Groups 2, 3, 4 experimental QI curves different from those predicted by using the "conversion" coefficients obtained from the data of Group 1.
To conclude this section, we recall that this procedure was adopted to verify whether, at least for a given fish species, a unique correspondence, through the conversion coefficients β_{1i}, β_{2i}, exists between spoilage bacteria concentrations and QIs scores. The results obtained seem to confirm this hypothesis, while indicating the presence of a behaviour qualitatively similar between predicted values and observed

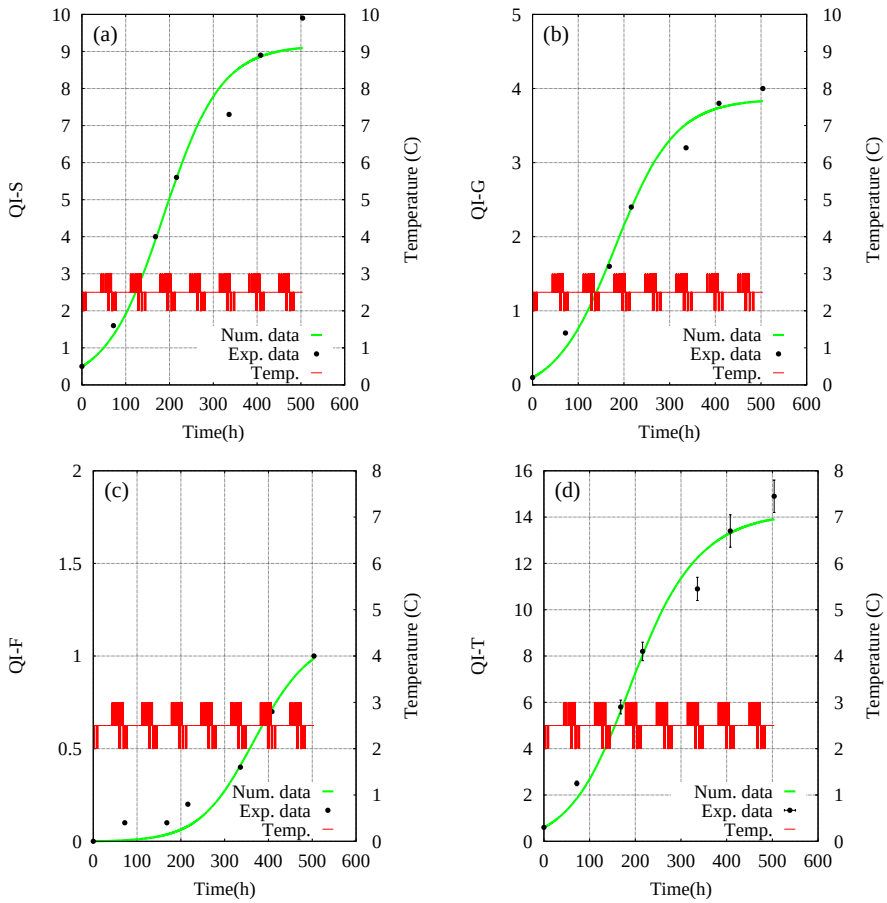

FIGURE 5. *Group 1. Comparison between observed (black dots) and predicted (green line) quality indexes: a) skin; b) gills; c) flesh. Panel d shows the total QI (summation of the scores obtained in the three sites). Vertical bars indicate experimental errors. Theoretical curves were calculated by Eqs. (3.1)-(3.3), setting* $\beta_{1S} = 0.01 \pm 0.01$, $\beta_{2S} = 1.39 \pm 0.01$, $\beta_{1G} = 0.01 \pm 0.01$, $\beta_{2G} = 0.70 \pm 0.01$, $\beta_{1F} = 0.33 \pm 0.01$, $\beta_{2F} = 0.16 \pm 0.01$. *These values were determined by a fitting procedure (minimization of the RMSE between sensory data and corresponding theoretical values). Red curves represent the temperature profiles.*

QIs scores also for Groups 2, 3, and 4.

5. Stochastic model

In this paragraph we analyze how random perturbations can affect the sensory evaluation performed by a panel of expert persons. As a starting point we consider the discrepancies between predicted values and observed QIs scores of Groups 2, 3, and 4 (see Figs. 6-8), and interpret them as a consequence of the uncertainty and variability, which can be present in sensory analysis. In fact, the results of a sensory evaluation depend also on the abilities of the expert persons that perform the analysis. Their skills can vary, in an unpredictable way, among different persons. Moreover, the same expert can evaluate differently the same fish sample, depending on the momentaneous conditions of his/her sensory abilities such as precision and reliability in evaluating surface and eyes appearance, odour, elasticity of muscle and gills. To take into account these "sources" of uncertainty and variability we modify our model by inserting terms of multiplicative noise in Eqs. (3.1)-(3.3). As a result, we obtain the following stochastic

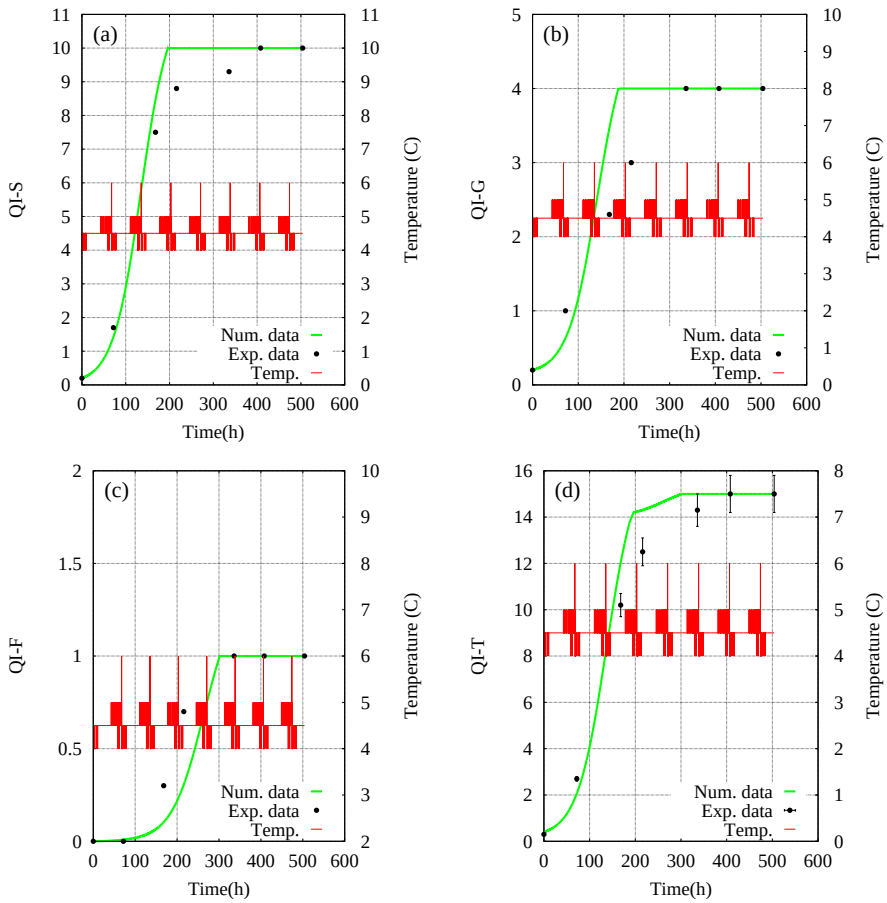

FIGURE 6. *Group 2. Comparison between observed (black dots) and predicted (green line) quality indexes for: a) skin; b) gills; c) flesh. Panel d shows the total QI (summation of the scores obtained in the three sites). Vertical bars indicate experimental errors. Theoretical curves were calculated from Eqs. (3.1)-(3.3), by using the same values of* β_{1i} *and* β_{2i} $(i = S, G, F)$ *as in Fig. 5. Red curves represent the temperature profiles.*

differential equations

$$\frac{dQI_S}{dt} = \frac{dN_{wS}}{dt}\beta_{1S} + \frac{dN_{bS}}{dt}\beta_{2S} + QI_S\,\xi_S \tag{5.1}$$

$$\frac{dQI_G}{dt} = \frac{dN_{wG}}{dt}\beta_{1G} + \frac{dN_{bG}}{dt}\beta_{2G} + QI_G\,\xi_G \tag{5.2}$$

$$\frac{dQI_F}{dt} = \frac{dN_{wF}}{dt}\beta_{1F} + \frac{dN_{bF}}{dt}\beta_{2F} + QI_F\,\xi_F, \tag{5.3}$$

where $\xi_i(t)$ are statistically independent Gaussian white noises with zero mean and correlation function $\langle \xi_i(t)\xi_j(t')\rangle = \sigma_i\delta(t-t')\delta_{ij}$ $(i,j = S,G,F)$.

5.1. Prediction of QIs values based on stochastic model

According to the deterministic study, the bacterial growth curves previously obtained (green lines in Figs. 1-4) are used in Eqs. (5.1)-(5.3), which are integrated numerically.
It is important to note that the use of a random function, i.e. noise source, to simulate the time behaviour of the system, makes the single realization unpredictable and unique, and therefore nonrepresentative of the real dynamics. As a consequence, one possible choice to describe correctly the time evolution of the

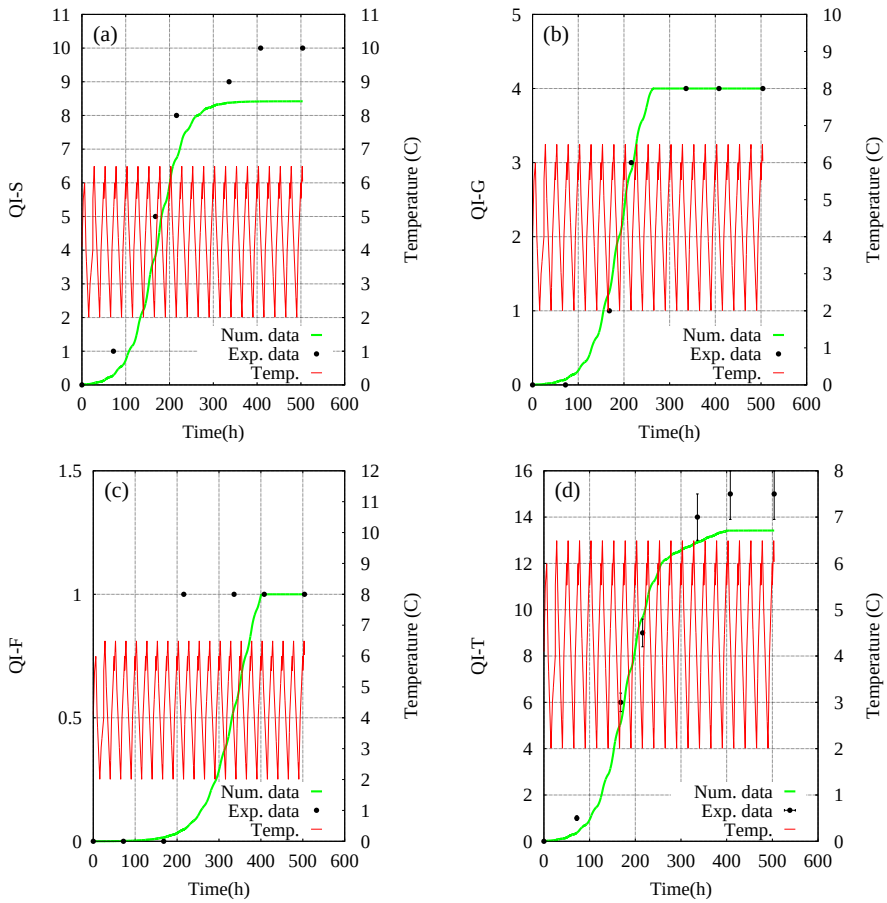

FIGURE 7. *Group 3. Comparison between observed (black dots) and predicted (green line) quality indexes for: a) skin; b) gills; c) flesh. Panel d shows the total QI (summation of the scores obtained in the three sites). Vertical bars indicate experimental errors. Theoretical curves were calculated from Eqs. (3.1)-(3.3), by using the same values of* β_{1i} *and* β_{2i} *(*$i = S, G, F$*) as in Fig. 5. Red curves represent the temperature profiles.*

system is to calculate the average of several realizations. This procedure, indeed, allows to take into account different trajectories obtained by the integration of the stochastic equations, without focusing on a specific realization [21]. Thus, the time behaviours of QIs is reproduced for different values of the three noise intensities (σ_S, σ_G, σ_F) by averaging over 1000 numerical realizations [22, 33]. For each group, the values of QIs predicted by the stochastic model are quantitatively compared with the observed QIs scores by using a minimization procedure based on the RMSE. Here we intend to focus on the predicted QIs characterized by a minimum of RMSE (best agreement with observed QIs). Therefore, as a preliminary analysis, in each site we obtain separately the theoretical QIs, while determining the noise intensity for which the RMSE is minimum. On the other side, it is reasonable to assume that, in each group, all three sites are subject to the same noise intensity. Therefore the total QI, including that corresponding to the minimum RMSE (best agreement), is calculated by setting the noise intensity to the same value in all three sites ($\sigma_S = \sigma_G = \sigma_F$). The results are given in Table 1. Here, for all groups, the noise intensity for which RMSE takes on the lowest value in each site is highlighted in green. The statistical analysis performed for Groups 1, 2, and 4 indicates that in most cases the agreement between predicted and observed partial QIs is better for noise intensities different from zero, that is when the stochastic approach is used.

Conversely, for Group 3 the RMSE becomes minimum for zero noise intensity on skin and flesh, and for

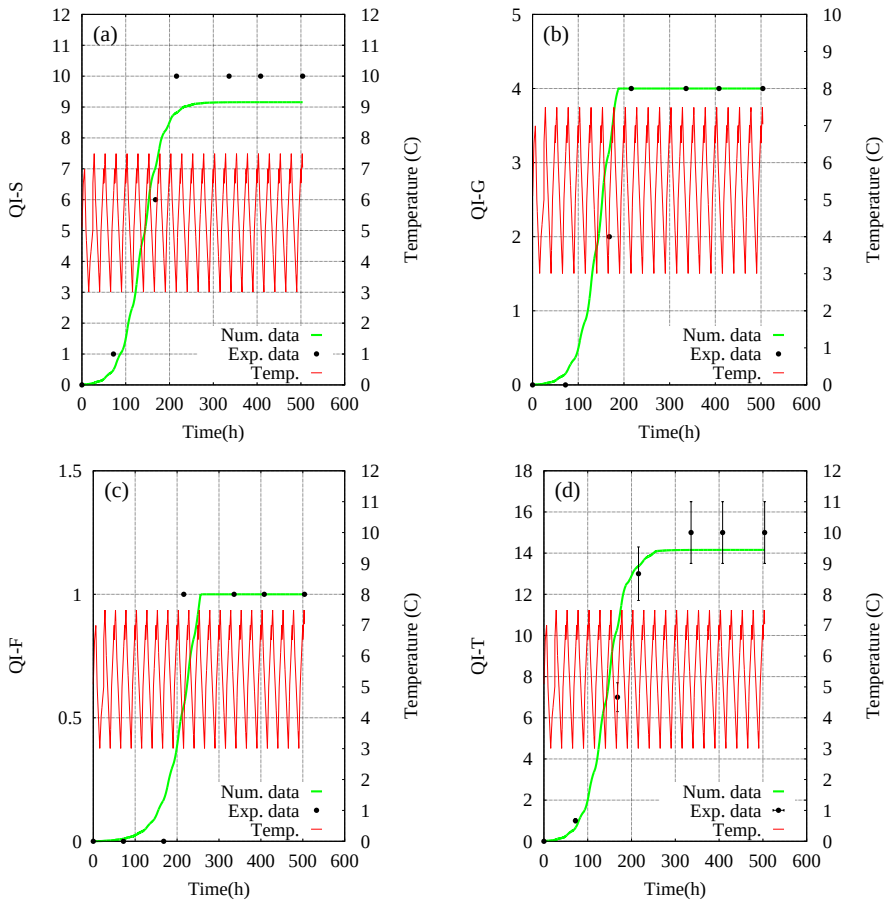

FIGURE 8. *Group 4. Comparison between observed (black dots) and predicted (green line) quality indexes for: a) skin; b) gills; c) flesh. Panel d shows the total QI (summation of the scores obtained in the three sites). Vertical bars indicate experimental errors. Theoretical curves were calculated from Eqs. (3.1)-(3.3), by using the same values of β_{1i} and β_{2i} $(i = S, G, F)$ as in Fig. 5. Red curves represent the temperature profiles.*

Group 1

Noise intensity	RMSE - QI SKIN	RMSE - QI GILLS	RMSE - QI FLESH	RMSE - QI TOTAL
0	0.541002	0.173015	0.067585	0.739064
0.000001	0.540118	0.172729	0.067589	0.737922
0.000002	0.539744	0.172725	0.067617	0.737775
0.000005	0.539014	0.173469	0.067709	0.738653
0.00001	0.538776	0.175208	0.06785	0.741245
0.00005	0.556157	0.188477	0.068798	0.774932
0.0001	0.577142	0.200374	0.06979	0.809138
0.001	0.753151	0.291912	0.08038	1.091611
0.01	1.298218	0.549239	0.118442	1.94918
0.1	2.05834	0.887655	0.168592	3.111489

Group 2

Noise intensity	RMSE - QI SKIN	RMSE - QI GILLS	RMSE - QI FLESH	RMSE - QI TOTAL
0	0.699217	0.643907	0.179713	1.118177
0.000001	0.699191	0.643888	0.179703	1.118135
0.00001	0.698936	0.643845	0.179682	1.117855
0.0001	0.666255	0.641304	0.179613	1.085707
0.0005	0.561648	0.612475	0.179528	0.961023
0.001	0.506358	0.583054	0.179712	0.880595
0.002	0.492968	0.549485	0.180646	0.844886
0.005	0.702034	0.512196	0.184329	1.05597
0.01	0.982917	0.520299	0.19113	1.424059
0.1	2.038678	0.77437	0.242373	2.948943

Group 3

Noise intensity	RMSE - QI SKIN	RMSE - QI GILLS	RMSE - QI FLESH	RMSE - QI TOTAL
0	1.214982	0.116786	0.432247	1.141956
0.000001	1.215018	0.116721	0.432258	1.142345
0.000002	1.215036	0.116694	0.432262	1.142512
0.000005	1.215079	0.11664	0.432271	1.142854
0.00001	1.215136	0.116579	0.432282	1.143285
0.00002	1.215531	0.116491	0.432296	1.144593
0.00005	1.22033	0.116386	0.432329	1.155167
0.0001	1.229694	0.117454	0.432379	1.180098
0.001	1.356704	0.181364	0.433481	1.459041
0.01	1.982934	0.476914	0.445529	2.422312
0.1	3.028511	0.887919	0.478072	3.900686

Group 4

Noise intensity	RMSE - QI SKIN	RMSE - QI GILLS	RMSE - QI FLESH	RMSE - QI TOTAL
0	0.902565	0.480286	0.196954	1.51523
0.000001	0.902511	0.480244	0.196933	1.515293
0.000002	0.902494	0.480226	0.196924	1.515322
0.000005	0.902558	0.480189	0.196907	1.515435
0.00001	0.903758	0.480146	0.196887	1.516233
0.0001	0.924738	0.479781	0.196737	1.527275
0.001	1.236484	0.478791	0.196347	1.716049
0.002	1.431365	0.483088	0.196727	1.869128
0.005	1.726684	0.496532	0.200325	2.131718
0.01	2.032876	0.534826	0.209121	2.451292
0.1	3.2[illegible]	0.[illegible]	0.[illegible]	3.789347

TABLE 5. *Root mean square error between observed QI scores and predicted values, calculated for different noise intensities, σ_S, σ_G, σ_F.*

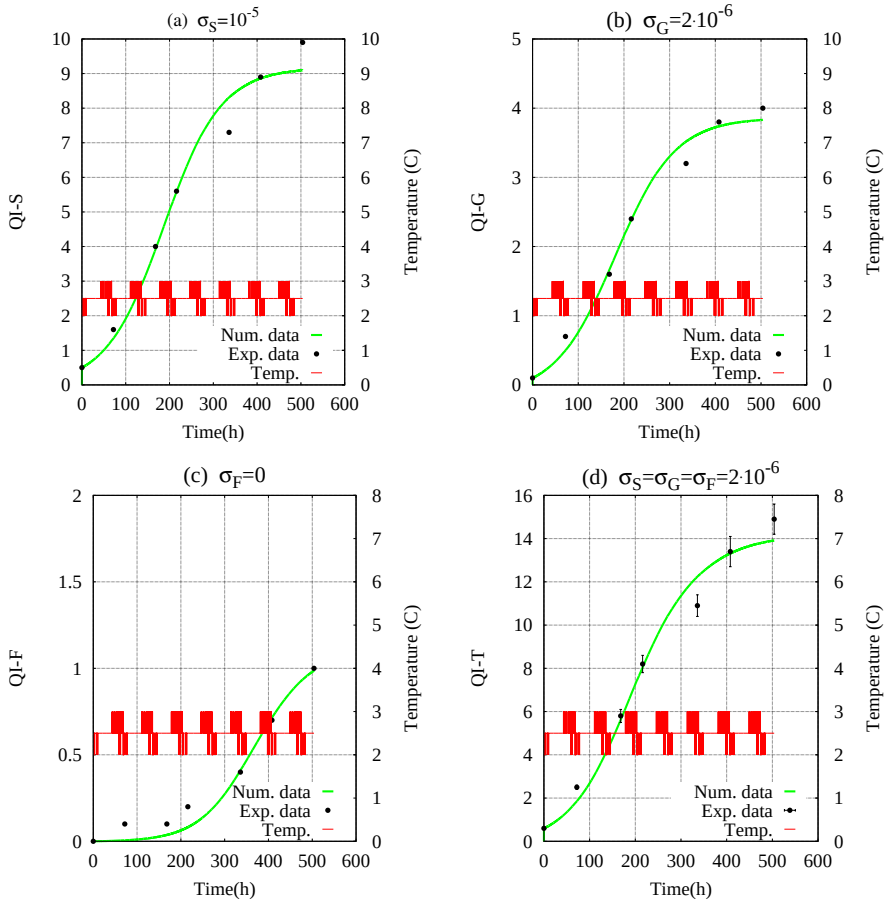

FIGURE 9. *Group 1. Comparison between observed (black dots) and predicted by stochastic model (green line) quality indexes: a) skin ($\sigma_S = 10^{-5}$); b) gills ($\sigma_G = 2 \cdot 10^{-6}$); c) flesh ($\sigma_F = 0$). Panel d shows the total QI ($\sigma_S = \sigma_G = \sigma_F = 2 \cdot 10^{-6}$). Vertical bars indicate experimental errors. Theoretical curves were calculated from Eqs. (5.1)-(5.3), by using the same values of β_{1i} and β_{2i} ($i = S, G, F$) as in Fig. 5. Red curves represent the temperature profiles.*

$\sigma_G = 5 \cdot 10^{-5}$ in gills.

Finally we note that for Groups 3 and 4 the minimum RMSE for the total QI is obtained when all three noise intensities are zero, that is in deterministic regime. This indicates that in the system analyzed the fluctuations connected with the uncertainty and variability of the sensory analysis affect weakly the QI evaluation.

The results of this section confirm that random perturbations influence in most case the QIs scores, and play therefore a non-negligible role in sensory analysis. These fluctuations can be interpreted as a consequence of uncertainty and variability in sensory analysis.

Figs. 9-12 show, for each group and site, the partial and total predicted QIs (green curves) for which the RMSE takes on the minimum value. As usual, black dots and red lines indicate observed QIs and temperature profiles, respectively. Note that curves obtained for zero noise intensity are those calculated by the deterministic model.

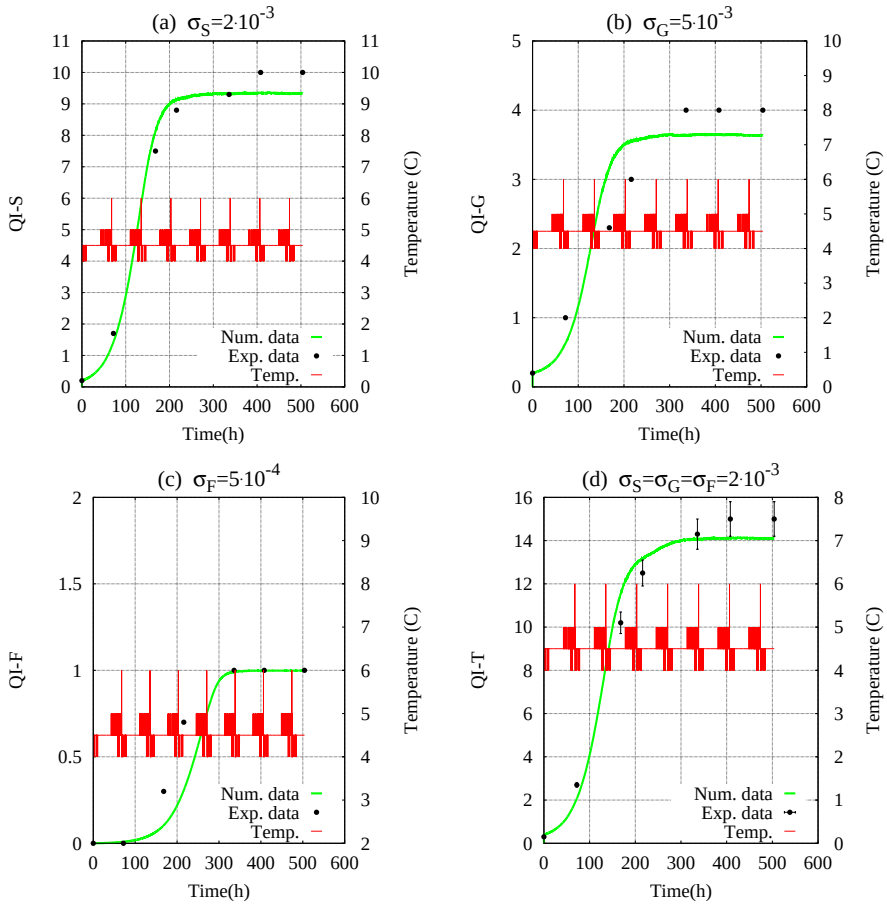

FIGURE 10. *Group 2. Comparison between observed (black dots) and predicted by stochastic model (green line) quality indexes: a) skin ($\sigma_S = 2 \cdot 10^{-3}$); b) gills ($\sigma_G = 5 \cdot 10^{-3}$); c) flesh ($\sigma_F = 5 \cdot 10^{-4}$). Panel d shows the total QI ($\sigma_S = \sigma_G = \sigma_F = 2 \cdot 10^{-3}$). Vertical bars indicate experimental errors. Theoretical curves were calculated from Eqs. (5.1)-(5.3), by using the same values of β_{1i} and β_{2i} $(i = S, G, F)$ as in Fig. 5. Red curves represent the temperature profiles.*

6. Conclusions

In this paper we studied a model which allows to reproduce the dynamics of two bacteria populations, Pseudomonas spp. and Shewanella spp., responsible for food spoilage. Specifically, we studied the dynamics of the two populations in specimens of Gilthead seabream (*Sparus aurata*), subdivided in four groups, by using a model based on two logistic equations, and analyzing separately the bacterial growths on skin, gills, and flesh.

By a fitting procedure we obtained theoretical growth curves for bacterial concentrations in a very good agreement with experimental data. As known, spoilage bacteria are responsible for loss of quality and freshness in fish products. Therefore we used theoretical growth curves for bacterial concentrations to predict the time behaviour of some sensory characteristics of the fish food analyzed. At this aim, we took into account the Quality Index Method (QIM), a scoring system for freshness and quality sensory estimation of fishery products, initially developed by the Tasmanian Food Research Unit [11]. The QIM scoring allows to assign demerit points to each sensory parameter considered, providing, by a summation of the partial scores, an overall sensory score named Quality Index (QI).
To analyze the connection between the sensory characteristics of fresh fish specimens and the two bacterial concentrations, we reproduced the QI scores observed in sensory analysis, by a set of differential equations,

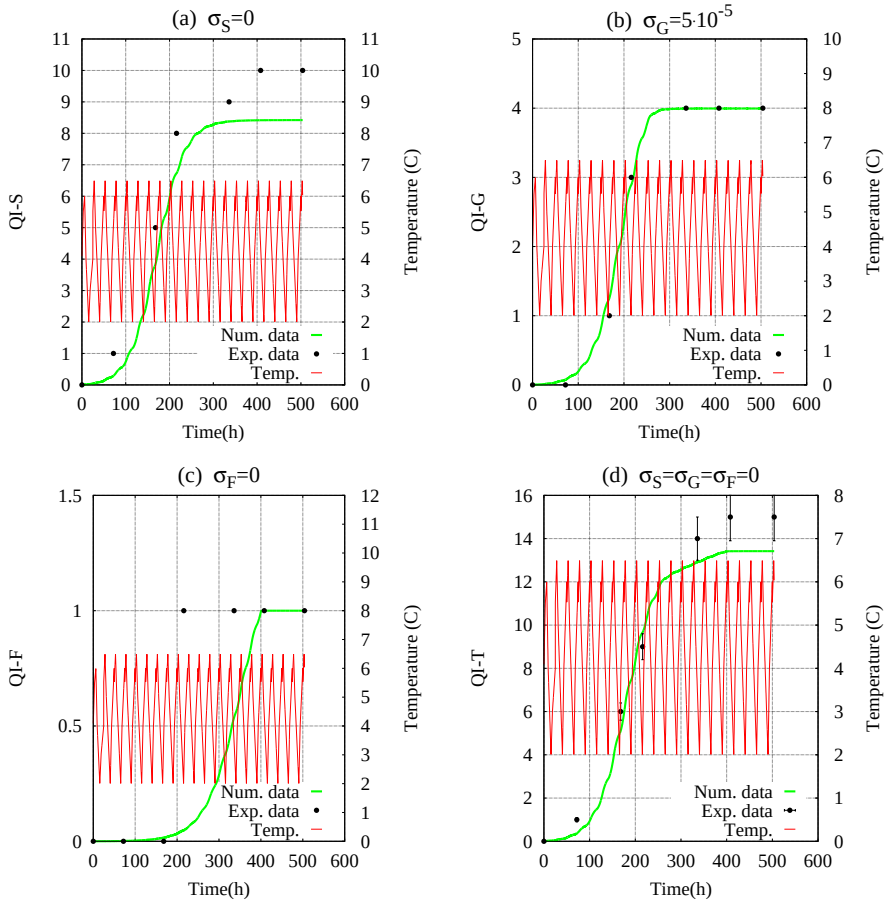

FIGURE 11. *Group 3. Comparison between observed (black dots) and predicted by stochastic model (green line) quality indexes: a) skin ($\sigma_S = 0$); b) gills ($\sigma_G = 5 \cdot 10^{-5}$); c) flesh ($\sigma_F = 0$). Panel d shows the total QI. ($\sigma_S = \sigma_G = \sigma_F = 0$). Vertical bars indicate experimental errors.* Theoretical curves were calculated from Eqs. (5.1)-(5.3), by using the same values of β_{1i} and β_{2i} $(i = S, G, F)$ as in Fig. 5. Red curves represent the temperature profiles.

which allow to "translate" the bacterial concentrations into QI scores. The investigation was carried out separately on skin, gills and flesh, obtaining a QI score for each site. In particular, we compared observed and predicted QIs. As a result, depending on the group of specimens considered and sites analyzed (skin, gills, or flesh), we found: i) a good agreement in all sites of Group 1, in flesh of Group 2, on gills of Group 3, in flesh and gills of Group 4; ii) a less good agreement in the other cases.

Finally, we took into account the effects of random fluctuations. Specifically, we considered uncertainty and variability in sensory analysis, by modeling them as effects of random fluctuations. Therefore, we modified the differential equations for QI scores by adding terms of multiplicative white Gaussian noise. By solving the equations of the stochastic model for different values of noise intensity, we obtained different QI curves. These were quantitatively compared with the experimental findings, coming from sensory analysis, by using the root mean square error test. We found that, for some groups of specimens considered and some sites analyzed (skin, gills, or flesh), theoretical QI scores obtained in the presence of suitable noise intensities are in a better agreement with those observed experimentally with respect to those calculated by the deterministic model.

Finally we note that our study could play a key role in view of using microbial predictive models not only for a food risk assessment, but also to develop a protocol which provides a quantitative estimation of the organoleptic properties of food products. Such a procedure, used together with experimental analyses

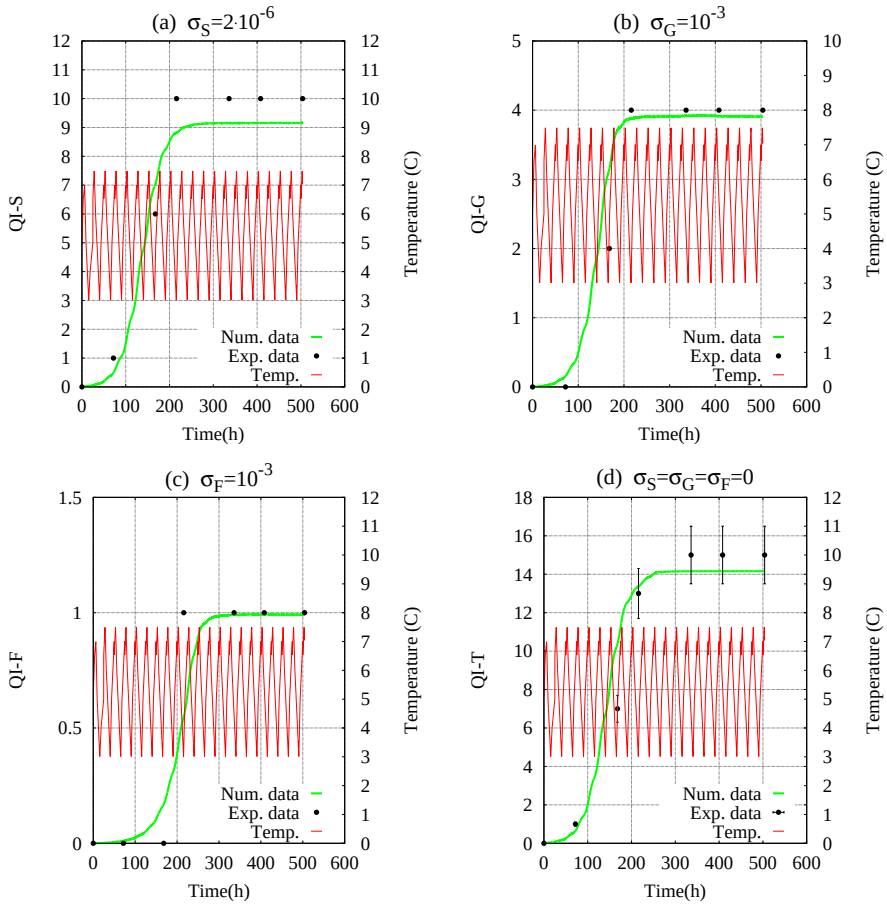

FIGURE 12. *Group 4. Comparison between observed (black dots)and predicted by stochastic model (green line) quality indexes: a) skin ($\sigma_S = 2 \cdot 10^{-6}$); b) gills ($\sigma_G = 10^{-3}$); c) flesh ($\sigma_F = 10^{-3}$). Panel d shows the total QI ($\sigma_S = \sigma_G = \sigma_F = 0$). Vertical bars indicate experimental errors. Theoretical curves were calculated from Eqs. (5.1)-(5.3), by using the same values of β_{1i} and β_{2i} $(i = S, G, F)$ as in Fig. 5. Red curves represent the temperature profiles.*

performed by "electronic noses", could permit to get a more trustable evaluation of the quality index, while contributing to make more precise the prediction of the changes occurring in the organoleptic properties. This aspect agrees to the new European approach to food quality assessment and management.

Acknowledgements

Authors acknowledge the financial support by Ministry of University, Research and Education of Italian Government, Project "RITMARE SP2_WP1_AZ3_UO04 - Potenziamento delle campagne scientifiche di acquisizione di informazioni indipendenti dalla pesca sulle risorse", and Project PON02_00451_3362121 "PESCATEC - Sviluppo di una Pesca Siciliana Sostenibile e Competitiva attraverso l'Innovazione Tecnologica".

References

[1] N. V. Agudov, A. A. Dubkov, B. Spagnolo, *Escape from a metastable state with fluctuating barrier.* Physica A, 325 (2003), 144–151.

[2] M. Asslani, F. Di Patti, D. Fanelli. *Stochastic Turing patterns on a network.* Phys. Rev. E, 86 (2012), 046105.

[3] G. Augello, D. Valenti, B. Spagnolo. *Non-Gaussian noise effects in the dynamics of a short overdamped Josephson junction.* Eur. Phys. J. B, 78 (2010), 225–234.

[4] J. Baranyi, T.A. Roberts. *A dynamic approach to predicting bacterial growth in food.* Int. J. Food Microbiol., 23 (1994), 277–294.

[5] J. Baranyi, T. P. Robinson, A. Kaloti, B. M. Mackey. *Predicting growth of Brochothrix thermosphacta at changing temperature.* Int. J. Food Microbiol., 27 (1995), 61–75.

[6] R. Benzi, A. Sutera, A. Vulpiani. *The mechanism of stochastic resonance.* J. Phys. A: Math Gen., 14 (1981), L453–L457.

[7] R. Benzi, G. Parisi, A. Sutera, A. Vulpiani. *Stochastic resonance in climatic change.* Tellus, 34 (1982), 10–16.

[8] T. Biancalani, D. Fanelli, F. Di Patti. *Stochastic Turing patterns in the Brusselator model.* Phys. Rev. E, 81 (2010), 046215.

[9] G. Bonanno, D. Valenti, B. Spagnolo. *Role of Noise in a Market Model with Stochastic Volatility.* Eur. Phys. J. B, 53 (2006), 405–409.

[10] G. Bonanno, D. Valenti, B. Spagnolo. *Mean Escape Time in a System with Stochastic Volatility.* Phys. Rev. E, 75 (2007), 016106.

[11] H. A. Bremner. *A convenient easy to use system for estimating the quality of chilled seafood.* In: Proceedings of the Fish Processing Conference, Nelson, New Zealand, 23–25 April 1985 (edited by D. N. Scott & C. Summers). Fish Processing Bulletin, 7 (1985), 59–703.

[12] J. H. Brown, T. G. Whitham, S. K. M. Ernest, C. A. Gehring. *Complex species interactions and the dynamics of ecological systems: long-term experiments.* Science, 293 (2001), 643–650.

[13] J. D. Challenger, D. Fanelli, A. J. McKane. *Intrinsic noise and discrete-time processes.* Phys. Rev. E, 88 (2013), 040102(R).

[14] O. Chichigina, D. Valenti, B. Spagnolo. *A Simple Noise Model with Memory for Biological Systems.* Fluct. Noise Lett., 5 (2005), L243–L250.

[15] O. A. Chichigina. *Noise with memory as a model of lemming cycles.* Eur. Phys. J. B, 65 (2008), 347–352.

[16] O. A. Chichigina, A. A. Dubkov, D. Valenti, B. Spagnolo. *Stability in a system subject to noise with regulated periodicity.* Phys. Rev. E, 84 (2011), 021134(1-10).

[17] S. Ciuchi, F. de Pasquale, B. Spagnolo. *Nonlinear Relaxation in the presence of an Absorbing Barrier.* Phys. Rev. E, 47 (1993), 3915–3926.

[18] P. Dalgaard, P. Buch, S. Silberg. *Seafood Spoilage Predictor–development and distribution of a product specific application software.* Int. J. Food Microbiol., 73 (2002), 343–349.

[19] T. Dauxois, F. Di Patti, D. Fanelli, A. J. McKane. *Enhanced stochastic oscillations in autocatalytic reactions.* Phys. Rev. E, 79 (2009), 036112.

[20] P. de Anna, F. Di Patti, D. Fanelli, A. J. McKane, T. Dauxois. *Spatial model of autocatalytic reactions.* Phys. Rev. E, 81 (2010), 056110.

[21] G. Denaro, D. Valenti, A. La Cognata, B. Spagnolo, A. Bonanno, G. Basilone, S. Mazzola, S. W. Zgozi, S. Aronica, C. Brunet. *Spatio-temporal behaviour of the deep chlorophyll maximum in Mediterranean Sea: Development of a stochastic model for picophytoplankton dynamics.* Ecol. Complex., 13 (2013), 21–34.

[22] G. Denaro, D. Valenti, B. Spagnolo, G. Basilone, S. Mazzola, S. W. Zgozi, S. Aronica, A. Bonanno. *Dynamics of two picophytoplankton groups in Mediterranean Sea: Analysis of the deep chlorophyll maximum by a stochastic advection-reaction-diffusion model.* PLoS ONE, 8 (2013), e66765.

[23] E. J. Dens, K. M. Vereecken, J. F. Van Impe. *A prototype model structure for mixed microbial populations in homogeneous food products.* J. Theor. Biol., 201 (1999), 159–170.

[24] A. Dubkov, B. Spagnolo. *Langevin Approach to Lévy flights in fixed potentials: Exact results for stationary probability distributions.* Acta Phys. Pol. B, 38 (2007), 1745–1758.

[25] A. Fiasconaro, D. Valenti, B. Spagnolo. *Role of the initial conditions on the enhancement of the escape time in static and fluctuating potentials* Physica A, 325 (2003), 136–143.

[26] A. Fiasconaro, D. Valenti, B. Spagnolo. *Nonmonotonic behavior of spatiotemporal pattern formation in a noisy Lotka-Volterra system.* Acta Phys. Pol. B, 35 (2004), 1491–1500.

[27] A. Fiasconaro, A. Ochab–Marcinek, B. Spagnolo, E. Gudowska–Nowak. *Monitoring noise–resonant effects in cancer growth influenced by external fluctuations and periodic treatment.* Eur. Phys. J. B, 65 (2008), 435–442.

[28] A. Fiasconaro, B. Spagnolo. *Resonant activation in piece-wise linear asymmetric potentials.* Phys. Rev. E, 83 (2011), 041122.

[29] J. A. Freund, T. Pöschel (Eds.). Stochastic Processes in Physics, Chemistry, and Biology. Lecture Notes in Physics 557, Springer, Berlin, 2000.

[30] L. Gammaitoni, P. Hänggi, P. Jung, F. Marchesoni. *Stochastic resonance.* Rev. Mod. Phys., 70 (1998), 223–287.

[31] A. Giuffrida, G. Ziino, D. D'Ambrosi, V. Mandalà, A. Panebianco. *Study on the transcutaneous bacterial migration in some fish species.* In: Proceeding of XV National Congress of Italian Association of Veterinary Hygienists, (2005) 279–282. Tirrenia, Italy: A.I.V.I.

[32] A. Giuffrida, G. Ziino, D. Valenti, G. Donato, A. Panebianco. *Application of an interspecific competition model to predict the growth of Aeromonas hydrophila on fish surfaces during refrigerated storage.* Archiv für Lebensmittelhygiene, 56 (2007), 136–141.

[33] A. Giuffrida, D. Valenti, G. Ziino, A. Panebianco, *Study on the application of an interspecific competition model for the prediction of the microflora behaviour during the fermentation process of S. Angelo PGI salami.* Vet. Res. Commun., 33 (2009), S229–S232.

[34] A. Giuffrida, D. Valenti, G. Ziino, B. Spagnolo, A. Panebianco. *A stochastic interspecific competition model to predict the behaviour of Listeria monocytogenes in the fermentation process of a traditional Sicilian salami.* Eur. Food Res. Technol., 228 (2009), 767–775.

[35] A. Giuffrida, D. Valenti, F. Giarratana, G. Ziino, A. Panebianco. *A new approach to modeling the shelf life of Gilthead seabream (Sparus aurata)* Int. J. Food Sci. Tech., 48 (2013), 1235–1242.

[36] C. Guarcello, D. Valenti, B. Spagnolo. *Phase dynamics in graphene-based Josephson junctions in the presence of thermal and correlated fluctuations.* Phys. Rev. B, 92 (2015), 174519.

[37] P. Hänggi, P. Talkner, M. Borkovec. *Reaction rate theory: fifty years after Kramers.* Rev. Mod. Phys., 62 (1990), 251–342.

[38] A. Huidobro, A. Pastor, M. Tejada. *Quality Index Method developed for raw Gilthead Seabream (Sparus aurata).* J. Food Sci., 65 (2000), 1202–1205.

[39] H. H. Huss. *Quality and Quality Changes in Fresh Fish.* FAO Fisheries Technical Paper, 348 (1995), 130–131. Rome, Italy: FAO.

[40] P. Jung, P. Hänggi. *Amplification of small signals via stochastic resonance.* Phys. Rev. A, 44 (1991), 8032–8042.

[41] K. Koutsoumanis, G. J. E. Nychas. *Application of a systematic experimental procedure to develop a microbial model for rapid fish shelf life predictions.* Int. J. Food Microbiol., 60 (2000), 171–184.

[42] A. La Barbera, B. Spagnolo. *Spatio-Temporal Patterns in Population Dynamics.* Physica A, 314 (2002), 120–124.

[43] A. La Cognata, D. Valenti, A. A. Dubkov, B. Spagnolo. *Dynamics of two competing species in the presence of Lévy noise sources.* Phys. Rev. E, 82 (2010), 011121.

[44] A. La Cognata, D. Valenti, B. Spagnolo, A. A. Dubkov. *Two competing species in super-diffusive dynamical regimes.* Eur. Phys. J. B, 77 (2010), 273–279.

[45] V. P. Lougovois, E. R. Kyranas, V. R. Kyrana. *Comparison of selected methods of assessing freshness quality and remaining storage life of iced Gilthead sea bream (Sparus aurata).* Food Res. Int., 36 (2003), 551–560.

[46] R. N. Mantegna, B. Spagnolo. *Stochastic Resonance in a Tunnel Diode.* Phys. Rev. E, 49 (1994), R1792–R1795.

[47] R. N. Mantegna, B. Spagnolo. *Probability distribution of the Residence Times in Periodically Fluctuating Metastable Systems.* Int. J. Bif. Chaos, 8 (1998), 783–790.

[48] R. N. Mantegna, B. Spagnolo, L. Testa, M. Trapanese. *Stochastic Resonance in Magnetic Systems described by Preisach Hysteresis Model.* J. Appl. Phys., 97 (2005), 10E519.

[49] K. Neumeyer, T. Ross, T.A. Mcmeekin. *Development of a predictive model to describe the effects of temperature and water activity on the growth of spoilage pseudomonads.* Int. J. Food Microbiol., 38 (1997), 45–54.

[50] E. L. Pankratov, B. Spagnolo. *Optimization of impurity profile for p-n junction in heterostructures.* Eur. Phys. J. B, 46 (2005), 15–19.

[51] C. Parra–Rojas, J. D. Challenger, D. Fanelli, A. J. McKane. *Intrinsic noise and two-dimensional maps: Quasicycles, quasiperiodicity, and chaos.* Phys. Rev. E, 90 (2014), 032135.

[52] D. Persano Adorno, N. Pizzolato, D. Valenti, B. Spagnolo. *External Noise Effects in doped semiconductors operating under sub-THz signals.* Rep. Math. Phys., 70 (2012), 171–179.

[53] D. A. Ratkowsky, R. K. Lowry, T. A. Mcmeekin, A. N. Stokes, R. E. Chandler. *Model for bacterial cultures growth rate throughout the entire biokinetic temperature range.* J. Bacteriology, 154 (1983), 1222–1226.

[54] T. Ross, P. Dalgaard. *Secondary models.* In: Modeling Microbial Responses in Foods (Eds. R. C. McKeller, X. Lu), pp. 63–150, CRC Press, Boca Raton, USA, 2003.

[55] D. F. Russel, L. A. Wilkens, F. Moss. *Use of behavioural stochastic resonance by paddle fish for feeding.* Nature, 402 (2000), 291–294.

[56] B. Spagnolo, A. Fiasconaro, D. Valenti. *Noise Induced Phenomena in Lotka-Volterra Systems.* Fluct. Noise Lett., 3 (2003), L177–L185.

[57] B. Spagnolo, D. Valenti. *Volatility effects on the escape time in financial market models.* Int. J. Bifurcation and Chaos, 18 (2008), 2775–2786.

[58] B. Spagnolo, S. Spezia, L. Curcio, N. Pizzolato, A. Fiasconaro, D. Valenti, P. Lo Bue, E. Peri, S. Colazza. *Noise effects in two different biological systems.* Eur. Phys. J. B, 69 (2009), 133–146.

[59] D. Valenti, A. Fiasconaro, B. Spagnolo. *Stochastic resonance and noise delayed extinction in a model of two competing species.* Physica A, 331 (2004), 477–486.

[60] D. Valenti, A. Fiasconaro, B. Spagnolo. *Pattern formation and spatial correlation induced by the noise in two competing species.* Acta Phys. Pol. B, 35 (2004), 1481–1489.

[61] D. Valenti, L. Schimansky-Geier, X. Sailer, B. Spagnolo. *Moment Equations for a Spatially Extended System of Two Competitive Species.* Eur. Phys. J. B, 50 (2006), 199-203.

[62] D. Valenti, B. Spagnolo, G. Bonanno. *Hitting Time Distributions in Financial Markets.* Physica A, 382 (2007), 311–320.

[63] D. Valenti, G. Augello, B. Spagnolo. *Dynamics of a FitzHugh-Nagumo system subjected to autocorrelated noise.* Eur. Phys. J. B, 65 (2008), 443–451.

[64] D. Valenti, G. Denaro, D. Persano Adorno, N. Pizzolato, S. Zammito, B. Spagnolo. *Monte Carlo analysis of polymer translocation with deterministic and noisy electric fields.* Cent. Eur. J. Phys., 10 (2012), 560–567 .

[65] D. Valenti, G. Denaro, A. La Cognata, B. Spagnolo, A. Bonanno, G. Basilone, S. Mazzola, S. Zgozi, S. Aronica. *Picophytoplankton dynamics in noisy marine environment.* Acta Phys. Pol. B, 43 (2012), 1227–1240.

[66] D. Valenti, C. Guarcello, B. Spagnolo. *Switching times in long-overlap Josephson junctions subject to thermal fluctuations and non-Gaussian noise sources.* Phys. Rev. B, 89 (2014), 214510.

[67] D. Valenti, L. Magazzù, P. Caldara, B. Spagnolo. *Stabilization of quantum metastable states by dissipation.* Phys. Rev. B, 91 (2015), 235412.

[68] D. Valenti, G. Denaro, B. Spagnolo, F. Conversano, C. Brunet. *How diffusivity, thermocline and incident light intensity modulate the dynamics of deep chlorophyll maximum in Tyrrhenian Sea.* PLoS ONE, 10 (2015), e0115468.

[69] R. C. Whiting, R. L. Buchanan. *A classification of models for predictive microbiology.* Food Microbiol., 10 (1993), 175–177.